Cu^{3+} Ion in Corundum

W. E. Blumberg, J. Eisinger, and S. Geschwind
Bell Telephone Laboratories, Murray Hill, New Jersey
(Received 30 November 1962)

The paramagnetic resonance spectrum of the ion Cu^{3+} (configuration $3d^8$ which is isoelectronic with Ni^{2+}) in Al_2O_3 has been studied. The results are correlated with the observed optical absorption spectrum in terms of crystal field theory. In addition, precise information about the electron-nuclear interactions of this ion was obtained by means of the electron nuclear double resonance (ENDOR) technique. The Cu^{3+} entered the Al_2O_3 lattice as a substitutional impurity for Al^{3+}. The ion exhibits a spectrum typical of a center with $S=1$ in an axially symmetrical site. Each electronic transition has four hyperfine components arising from a nuclear spin of 3/2. The lines corresponding to the two isotopes Cu^{63} and Cu^{65} were unresolved in the paramagnetic spectrum. The observed transitions yielded the following parameters: $D=-0.18838 \pm 0.00004$ cm^{-1}, $g_{\parallel}=2.0784\pm0.0005$, and $g_{\perp}=2.0772\pm0.0005$. In ENDOR experiments at 1.3°K, $\Delta m_s=0$, $\Delta m_I=\pm1$ transitions were observed with linewidths of about 50 kc/sec. These could be fitted satisfactorily only by postulating an effective field at the nucleus equal to $(1+\delta)H_0$, where H_0 is the external field and $\delta=0.0087$. Other interaction parameters are $A_{63}=-192.947\pm0.001$ Mc/sec; $A_{65}=-206.679\pm0.001$ Mc/sec; $B_{63}=-180.10\pm0.05$; $B_{65}=-192.916\pm0.05$; $e^2qQ_{63}=-0.168\pm0.004$ Mc/sec. From the magnitude of δ, an estimate is made of $\langle 1/r^3\rangle$ of Cu^{3+}. The surprisingly small value of e^2qQ is also discussed. The hyperfine structure anomaly $(A_{63}/A_{65})(g_{65}/g_{63})-1=(0.0145\pm0.0020)$ %. Since this agrees with the value obtained for $s_{1/2}$ electrons in Cu as measured by atomic beam magnetic resonance, one may conclude that the hyperfine interaction in Cu^{3+} has its major origin in $s_{1/2}$ electrons polarized by s-d interactions.

I. INTRODUCTION

FROM the point of view of crystal field theory, the study of different magnetic ions in the same host crystal offers the most direct way of observing the difference between the ions. The stability of corundum and the ease with which so many of the transition metal ions can be incorporated into the lattice as impurities make it an ideal crystal in this respect.

In this paper, we present the results of optical, paramagnetic resonance (EPR), and electron nuclear double resonance (ENDOR) experiments on Cu^{3+} in α-Al_2O_3. This is the first time that such spectra of Cu^{3+} have been observed in any host substance and the interest in these results is enhanced by a comparison with the isoelectronic Ni^{2+} in the same crystal which has previously been reported on.[1,2] In addition, very precise information on the electron nuclear interaction is obtained from the ENDOR spectrum.

Cu^{3+} has the configuration $3d^8$ and its ground-state free-ion term is a ^3F, with $L=3$ and $S=1$. In corundum it substitutes for Al^{3+} which is in sixfold oxygen coordination. The crystalline electric field acting upon the Cu^{3+} is predominantly cubic upon which is superimposed a smaller trigonal field, the site symmetry being C_3. The cubic crystal field lifts the sevenfold orbital degeneracy of the free-ion ^3F term into a lower singlet, $^3A_2$ and two triplets $^3T_2$ and $^3T_1$ as shown in Fig. 1. The combined action of the trigonal field and spin orbit (s-o) coupling lifts the remaining spin degeneracy of the ground-state $^3A_2$ level into a singlet ($m_s=0$) and a doublet ($m_s=\pm1$), between which levels the paramagnetic resonance absorptions are observed. The details of the magnetic properties of the $^3A_2$ ground state depend upon the mixing into the ground state, by s-o coupling, of the higher crystalline field levels (primarily the $^3T_2$). It is, therefore, important to locate these excited states by studying the optical absorption spectrum of Cu^{3+} in this crystal.

In Sec. II, we describe the samples and the experimental apparatus used. In Sec. III, the paramagnetic resonance results are presented. They are interpreted in Sec. IV in terms of crystal field theory using the observed optical absorption spectrum. A comparison is made with Ni^{2+} and the trigonal field parameter, deduced from the electron spin resonance (ESR) results, is discussed. Finally in Sec. V the ENDOR results for Cu^{63} and Cu^{65} are given, from which the effective

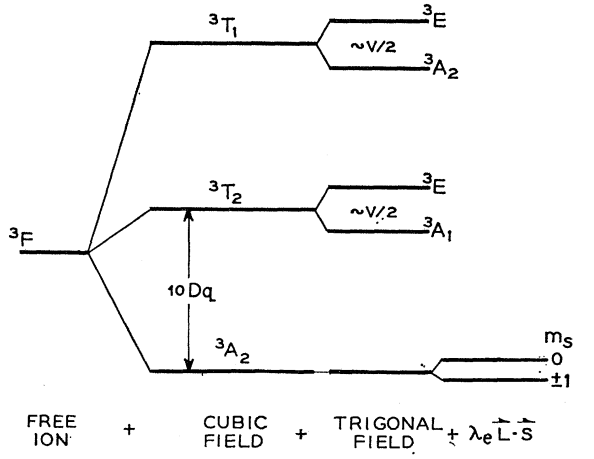

FIG. 1. Successive splitting of the free-ion ^3F level of $3d^8$ by a cubic field, trigonal field, and spin-orbit coupling. The order of the E and A levels for $^3T_2$ and $^3T_1$ is drawn to coincide with the negative value of D observed for the ground-state splitting as shown, as well as for the experimental observation $g_{\parallel}>g_{\perp}$, assuming isotropic s-o coupling. This corresponds, however, to a negative value of v as defined in the text.

[1] S. A. Marshall, Bull. Am. Phys. Soc. 5, 158 (1960).
[2] S. A. Marshall, T. T. Kikuchi, and A. R. Reinberg, Phys. Rev. 125, 453 (1962).

nuclear g factors, hyperfine interaction constants, and quadrupole coupling constants are found to very high precision. These results are discussed in Sec. VII. This discussion also makes use of the hyperfine structure anomaly arising from a difference in the magnetization distributions in the Cu^{63} and Cu^{65} nuclei and represents a novel tool in the investigation of the electronic wave functions of paramagnetic centers.

II. SAMPLES AND APPARATUS

The single crystals of Al_2O_3 used were grown by J. P. Remeika from oxide fluxes to which has been added a small amount of CuO. All the Cu entered the corundum lattice in the trivalent state (no Cu^{2+} was observed) and final concentrations of Cu^{3+} in samples from different batches ranged from a few parts in 10^4 to 10^5. As the spectrum displayed axial symmetry the Cu^{3+} presumably entered substitutionally for the Al^{3+}. While there are vacancies which are coordinated octahedrally by oxygen and have axial symmetry C_{3i} into which the Cu^{3+} might enter, one would assume that from a charge-balance point of view it is energetically more favorable for the Cu^{3+} to substitute for the Al^{3+}.

When the crystals were heated in a hydrogen atmosphere at 1200°C for several hours, all the Cu^{3+} was reduced to Cu^{2+}. This was made evident by the disappearance of the Cu^{3+} spectrum described below and by the appearance of a Cu^{2+} spectrum which showed Jahn-Teller effects[3] and which will be described in greater detail in a subsequent publication.

The crystals contained Fe^{3+} as an unintentional impurity at a level of a few parts in 10^4. This served as a convenient reference for checking the orientation of the crystals for ENDOR work *in situ*.

The paramagnetic resonance spectrometer used when not studying ENDOR utilized a matched cavity with superheterodyne detection and phase-sensitive detection at the i.f. frequency. A more detailed description of this spectrometer is to be found elsewhere.[4]

The ENDOR experiments were performed on a different K-band spectrometer which is very similar in construction to the X-band spectrometer described by Feher.[5] It employs two stabilized klystron signal generators supplied by Laboratory for Electronics, which are tunable over a frequency range of approximately 10%.

The rf magnetic field, H_2, necessary for the ENDOR experiments was provided by a two-turn coil outside a rectangular silver-coated glass cavity which resonated at 24 000 Mc/sec in the TE_{101} mode. Slots in the silver coating prevented the samples from being shielded from H_2. The rf current was supplied by two wideband amplifiers driven by Hewlett-Packard 608C oscillator whose tuning condenser could be slowly driven by a motor to scan the ENDOR frequency ν_E. ENDOR lines were recorded on a two-channel Sanborn recorder by raising or lowering ν_E and recording the χ' microwave signal on one channel while the other channel displayed a ν_E frequency analog. The microwave signal was detected by a superheterodyne detector with an i.f. of 60 Mc/sec. The frequency analog signal was obtained from a Hewlett-Packard 524C counter and digital-analog converter. Figure 2 illustrates the curves obtained in this manner.

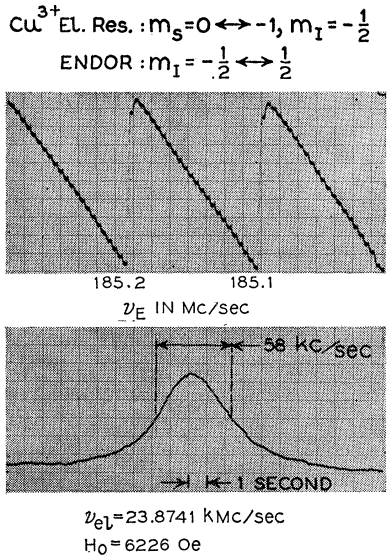

FIG. 2. The lower trace shows the ENDOR line corresponding to the transition $m_I=-\frac{1}{2}\rightarrow+\frac{1}{2}$ for the electronic level $m_s=-1$. The upper trace shows the analog of the rf frequency applied to the sample. The two traces were obtained simultaneously on a two-channel recorder.

All ENDOR measurements were obtained with the horizontal external field parallel to the c axis of the corundum crystal. This alignment presented no difficulty as far as the horizontal plane is concerned since the magnet could be rotated and the optimum orientation determined by observing one of the Cu^{3+} or Fe^{3+} impurity microwave lines as a function of angle. The azimuthal angle could not be conveniently varied continuously but an alignment check could be made to within about half a degree by using a mirror mounted parallel to the sample on the outside of the cavity to reflect a light beam. All ENDOR experiments were performed at 1.4°K.

The optical absorption spectra were obtained on a Carey Model 14 spectrophotometer.

III. PARAMAGNETIC RESONANCE SPECTRUM

The spin Hamiltonian for the $S=1$, $^3A_2$ ground state of Cu^{3+} appropriate to the axial symmetry of the site, with the z axis chosen to coincide with the c axis of the crystal, is

$$\begin{aligned}\mathcal{H}=&D[S_z^2-\tfrac{1}{3}S(S+1)]+g_{11}\beta H_0 S_z\cos\theta\\&+\tfrac{1}{2}g_\perp\beta H_0(S_+ +S_-)\sin\theta+AI_zS_z\\&+\tfrac{1}{2}B(S_+I_- +S_-I_+)-g_I{}^{11}\beta_N I_z H_0\cos\theta\\&-\tfrac{1}{2}g_I{}^{1}\beta_N H_0(I_+ +I_-)\sin\theta\\&+\{3e^2qQ/[4I(2I-1)]\}[I_z^2-\tfrac{1}{3}I(I+1)]. \quad (1)\end{aligned}$$

[3] S. Geschwind and J. P. Remeika, Suppl. J. Appl. Phys. **33**, 370 (1962).
[4] S. Geschwind, Phys. Rev. **121**, 363 (1961).
[5] G. Feher, Bell System Tech. J. **26**, 449 (1957).

The D term represents the lifting of the spin degeneracy of the ion in its ground state by the axial crystal field. The next two terms represent the Zeeman interaction of the electrons with the external field H_0. The A and B terms correspond to the electron-nuclear magnetic hyperfine interaction. The terms in β_N express the interaction between the effective magnetic moment of the nucleus and the external magnetic field. The need for using different symbols ($g_I^{\parallel}$ and $g_I^{\perp}$) for the nuclear g factors parallel and perpendicular to H_0 arises from the pseudofield effect (see Sec. VII.3) which is different for these two directions. The last term corresponds to the interaction between the nuclear electric quadrupole moment Q and the gradient of the electric field at the nucleus, q. The remaining operator and quantum number symbols have their usual meanings.

With the external magnetic field along the c axis the selection rules for the microwave transitions are normally $\Delta m_S=\pm 1$ and $\Delta m_I=0$. The hyperfine term $\frac{1}{2}B(S_+I_-+S_-I_+)$ connects m_S states separated by $\Delta m_S=\pm 1$. As a result, for example, the $m_S=\pm 1$ state will have some $m_S=0$ mixed into it so that even when H_0 is parallel to the c axis, the transition $m_S=+1\rightarrow -1$ is not completely forbidden. The intensity of these $m_S=\pm 2$ transitions relative to the $m_S=\pm 1$ transitions with H_0 along the c axis will be of the order $(B/g\beta H_0)^2$ and so are not a prominent feature of the "parallel" spectrum. With H_0 parallel to the c axis we, therefore, expect to see two groups of four lines corresponding to the $m_S=-1\rightarrow 0$ and $0\rightarrow +1$ transitions and the four nuclear substates of the copper with spin $I=3/2$. The positions of these lines including second-order corrections are given by

$$H_{-1\rightarrow 0}=H_0+D-Am_I-\frac{B^2}{2g_\perp\beta H}\left(\frac{15}{4}-m_I^2-m_I\right),$$
$$H_{0\rightarrow +1}=H_0-D-Am_I-\frac{B^2}{2g_\perp\beta H}\left(\frac{15}{4}-m_I^2+m_I\right), \quad (2)$$

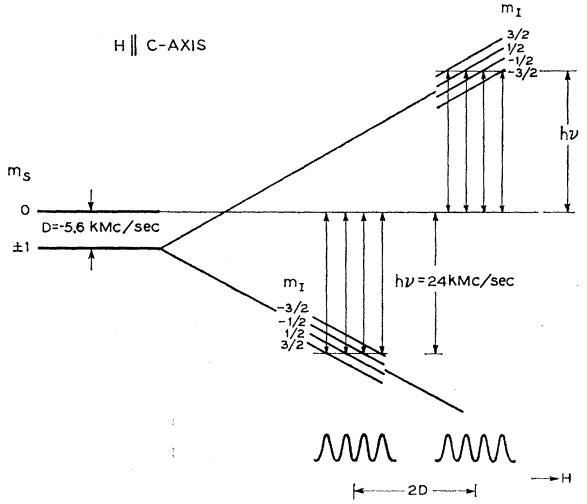

FIG. 3. Illustration of first order allowed ESR spectrum of Cu^{3+} with hfs, for H_0 parallel to the c axis.

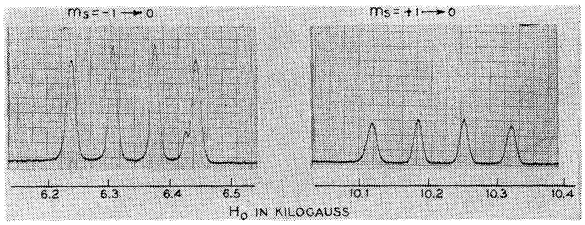

FIG. 4. Observed spectrum of Cu^{3+} at 1.8°K. The greater intensity of the low-field lines establishes the negative sign of D. At room temperature, the high- and low-field sets of lines had the same intensity. The weak line at 6.43 kG is due to iron impurities.

and are shown schematically in Fig. 3. The spectrum observed at 1.8°K is shown in Fig. 4. The greater intensity and smaller linewidth of the two central lines compared to the two outer lines of each hfs group are due to the unresolved lines of the two Cu isotopes whose moments differ by approximately 7% as shown in Fig. 5. The sign of D is determined in conventional fashion by comparing the intensity of $m_S=-1\rightarrow 0$ and $m_S=0\rightarrow +1$ transitions at low temperature. The increase in intensity of the low-field line in Fig. 4 establishes this as the $-1\rightarrow 0$ transition and from Eq. (1) D is, therefore, negative.

From observations on the spectrum with H_0 at right angles to the c axis ($\theta=90°$), B and $g_\perp$ can be obtained. While in principle e^2qQ can be found from the microwave measurements at angles intermediate between $\theta=0°$ and $\theta=90°$, its value was so small that no information about it could be obtained from the microwave measurements. However, a precise determination of e^2qQ was made from the ENDOR spectrum which is described below. The final results of the microwave measurements are listed in Table I. Considerably more accurate values of the hyperfine coupling constants are given below in the section on the ENDOR spectrum.

The signs of A and B relative to the sign of D are found from the second-order shifts in the hfs spacings. Equation (1) shows that if A and D have the same sign, the high-field intervals should be smaller than the corresponding low-field intervals. Since D was found to be negative, so must A be. This is also found to be the case for B. These signs are confirmed by ENDOR experiments.

TABLE I. A comparison of paramagnetic resonance data and derived quantities for Cu^{3+} and Ni^{2+} in Al_2O_3.

	Cu^{3+}	Ni^{2+} [a]
Dq	2100 cm^{-1}	~1000 cm^{-1} [b]
$g_\parallel$	2.0788±0.0005	2.196
$g_\perp$	2.0772±0.0005	2.187
$g_\parallel-g_\perp$	0.0016	0.009
D	−0.1884 cm^{-1}	−1.312 cm^{-1}
A^{63}	−193 Mc/sec±3	···
B^{63}	−180 Mc/sec±4	···
λ_e	−214 cm^{-1}	−240 cm^{-1}
λ_e/λ_0	0.51	0.74

[a] See references 1 and 2.
[b] See references 7 and 8 for optical data on Ni^{2+} in MgO. Dq for Ni^{2+} in Al_2O_3 was estimated from this data.

IV. DISCUSSION OF EPR RESULTS

We now wish to relate the experimental parameters in the spin Hamiltonian, such as the g values and the axial crystal field splitting, D, with the position and properties of the excited states of the Cu^{3+} ion in the crystal and compare these with Ni^{2+}. In Fig. 6 is shown a portion of Tanabe and Sugano's[6] energy level diagram for the d^8 configuration in a cubic field. For the sake of simplicity certain of the levels which are not relevant to our problem have been omitted. The splittings are plotted as a function of the cubic field parameter Dq and the diagram is normalized in terms of one of the Racah parameters B which measures the Coulomb interaction between the electrons. Following Tanabe and Sugano, the other Racah parameter C is taken as $B/4.71$, i.e., $\gamma=B/C=4.71$. To the right of the diagram is plotted the observed optical absorption spectrum of Cu^{3+} in Al_2O_3 and it is seen that the three observed peaks coincide very nicely with a Dq/B value of approximately 2.2.

The optical absorption spectrum of Ni^{2+} in α-Al_2O_3 has not been measured as it is obscured by the much stronger Ni^{3+} spectrum which is also present. However, one would not expect it to be very much different from that of Ni^{2+} in MgO [7,8] as both cases are characterized by sixfold octahedral oxygen coordination. It is estimated that Dq for Ni^{2+} will be slightly larger in Al_2O_3 as compared to MgO as the oxygen-metal ion distance is slightly smaller in Al_2O_3. The larger value of Dq for Cu^{3+} as compared to Ni^{2+} is in accord with the general empirical observation that Dq for trivalent ions is anywhere from 50 to 100% greater than for divalent ions.[9] This is generally explained as due to the fact that the central ion with the greater charge pulls the ligands closer in so that it sees a stronger crystal field.

The only level shown that is coupled to the ground state by s-o coupling is the $^3T_2$ (i.e., L transforms as T_1 and neither $E\times T_1$ nor $T_1\times T_1$ contain A_2). Thus, the greater $^3A_2\rightarrow{}^3T_2$ separation for the Cu^{3+} compared to Ni^{2+} will cause the g value of Cu^{3+} to be closer to the spin-only value of 2 and its ground-state splitting will be smaller as seen in Table I.

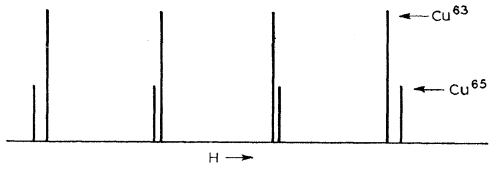

FIG. 5. An illustration of how the different moments of the two Cu isotopes broaden and lower the peak intensities of the two outer hfs components relative to the two center ones.

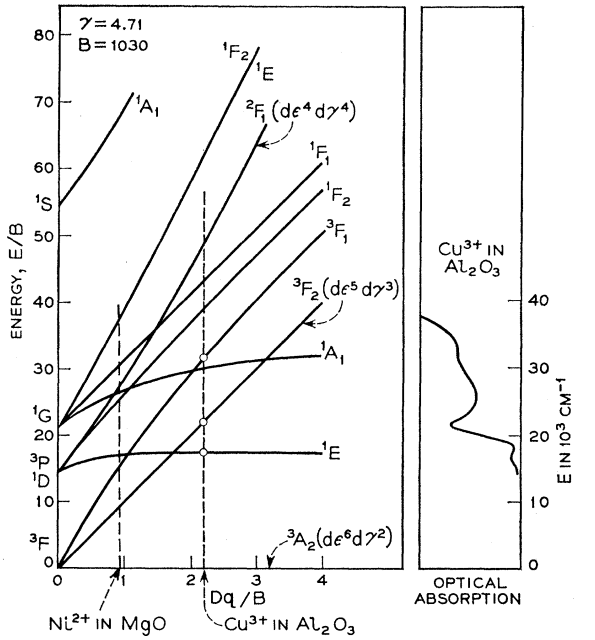

FIG. 6. A portion of Tanabe and Sugano's energy level diagram for d^8, where for simplicity's sake certain of the levels not relevant to our problem have been omitted. To the right of the diagram is plotted the optical absorption observed by D. L. Wood and the authors for Cu^{3+} in Al_2O_3, which coincides with a Dq/B value of 2. In contrast, the crystal field splitting for Ni^{2+} is estimated to be half as great.

Under the action of the trigonal field, the T_2 and T_1 levels are each split into an orbital doublet E and singlet A whose relative positions are determined by the sign of the axial crystal field.

The sign and magnitude of the trigonal field may be expressed in terms of the action of the trigonal field upon a single d electron in a t_2 orbital. The trigonal field splits a t_2 orbital into a doublet and singlet whose separation we call v and the sign of v is taken to be positive if the doublet is lower (following Pryce and Runciman[10]). The effect of the trigonal field upon an energy level of an ion with more than one d electron can always be expressed in terms of this one electron parameter v.

Thus, considering perturbations from the $^3T_2$ level only, the ground-state g values and axial crystal field splitting are given by[11–13]

$$g_{\parallel}=g_e-\frac{8\lambda_e}{E(^3A_1)-E(^3A_2)}, \tag{3}$$

$$g_{\perp}=g_e-\frac{8\lambda_e}{E(^3E)-E(^3A_2)}, \tag{4}$$

[6] Y. Tanabe and S. Sugano, J. Phys. Soc. Japan **9**, 753, 766 (1954).
[7] W. Low, Phys. Rev. **109**, 247 (1958).
[8] R. Pappalardo, D. L. Wood, and R. Linares, Jr., J. Chem. Phys. **35**, 1460 (1961).
[9] See Table VII of D. S. McClure, *Progress in Solid State Physics* (Academic Press Inc., New York, 1959), Vol. 9.
[10] M. H. L. Pryce and W. A. Runciman, Discussions Faraday Soc. **26**, 24 (1958).
[11] A. Abragam and H. M. L. Pryce, Proc. Roy. Soc. (London) **A205**, 135 (1951).
[12] G. Emch and R. Lacroix, Helv. Phys. Acta **33**, 1021 (1960).
[13] J. E. Geusic, thesis, Ohio State University, 1958 (unpublished).

$$D=-4\lambda_e^2\frac{E(^3E)-E(^3A_1)}{[E(^3A_1)-E(^3A_2)][E(^3E)-E(^3A_2)]}$$
$$=\tfrac{1}{2}\lambda(g_{\parallel}-g_{\perp}). \quad (5)$$

In the strong crystal field limit where $E(^3E)-E(^3A_1)=v/2$, one has

$$D\approx-\frac{2\lambda_e^2 v}{[E(^3T_2)-E(^3A_2)]^2}. \quad (6)$$

Here g_e is the free-electron g factor and λ_e is the effective spin-orbit coupling constant in the crystal into which the orbital reduction factor k_{ij}' has been absorbed.[14] λ_e is reduced from the free-ion value λ_0 as seen from the last row of Table I.

The splitting of the $^3T_2$ level is not observed optically as the band is very broad. Also, there was no significant dichroic shift in this band (as is found in ruby, for example[3,9,15]) from which this splitting might be deduced. This is undoubtedly due to the fact that there is a further splitting of the ^3E and ^3A levels by s-o coupling which is comparable to the trigonal field splitting. However, the s-o splitting in the excited states should have a negligible effect on the ground-state properties such as the D splitting. Thus, the average position of the $^3T_2\rightarrow{}^3A_2$ band is used in Eq. (6) to determine λ_e from the measured g shifts and is given in Table I.

Having thus determined λ_e it may be used to determine the trigonal field parameter v from Eq. (6) using the measured D value. One finds $v=-1030$ cm^{-1} for Cu^{3+} and $v=-1100$ cm^{-1} for Ni^{2+}. Here one encounters the difficulty that the value of v so determined has the opposite sign to that found for many other ions in corundum as already indicated elsewhere.[3] There are a number of possible explanations for this difficulty. Several of these will now be discussed.

A. Movement of the Ion

While the Cu^{3+} ion enters substitutionally for Al^{3+}, it may be displaced axially from the precise Al^{3+} position. The trigonal field is fairly sensitive to such an axial displacement: Point charge calculations indicate that an axial displacement of only 5% from the Al^{3+} position could change the sign of the trigonal field. Evidence for such a displacement has been claimed recently from an analysis of optical spectra of transition metal ions in corundum,[16] as well as from the ENDOR spectrum of Cr^{3+} in Al_2O_3 in which the quadrupole coupling constants of near neighbor Al nuclei were observed to be different than for the bulk of Al nuclei.[17] However, in these cases the possibility of such a motion of the ion was used to explain the observed *positive* v, which is opposite in sign to what a point-charge calculation predicted. One may seriously question the validity of such a point-charge calculation even with regard to sign. While there were some variations of the magnitude of v deduced from the optical spectra of different ions,[17] all values of v were positive.

B. The Role of Excited States other than $^3T_2$

The assumption that the $^3T_2$ is the only excited state that contributes to the ground-state splitting may be invalid, i.e., Eqs. (1), (2), and (4) may be inadequate. It should be noted that one encounters the same difficulty in the ground-state splitting of Cr^{3+} in Al_2O_3 where an incorrect sign of D is predicted if one uses a positive v and considers only the coupling to the excited $^4T_2$ state.[18] Sugano and Peter,[19] in an extensive calculation, obtained the correct sign of D using a positive v by taking into account configuration mixing of higher excited states as well as covalency but the absolute value of D they calculated still differed by some 30% from the measured value.

Along similar lines Lacroix[20] has indicated how a more complete molecular orbital treatment suggests the inadequacy of considering only the $^4T_2(t_2^3)$ state and that there are charge-transfer states of symmetry $^4T_2$ which might be important in determining the properties of the $^4A_2$ ground state.

C. Anisotropic s-o Coupling

Sugano and Tanabe,[18] in trying to explain the discrepancy between the observed sign of the ground-state splitting, D, of Cr^{3+} in Al_2O_3 and the positive sign of v as deduced from the dichroism of the ruby optical spectrum, first suggested the important role that anisotropic spin-orbit coupling could play. If one confines oneself to crystal field states arising from the same free-ion term, then the anisotropic s-o coupling can be represented by

$$\lambda_{\parallel}'L_zS_z+\lambda_{\perp}'(L_xS_x+L_yS_y). \quad (7)$$

Here λ' is the effective s-o coupling constant in the crystal including all orbital reduction and covalent effects so that matrix elements of L are taken between pure d orbitals. Similarly k' is the orbital reduction factor for angular momentum, i.e., $k'=|e|L|t_2|$, where e and t_2 are molecular orbitals. With this anisotropy,

[14] Λ_{ij} with overlap $=(k_{ij}')^2\cdot(\Lambda_{ij}$ for unmodified d orbitals), so that our $\lambda_e=\lambda''k'^2$, where λ'' includes the reduction of $\langle 1/r^3\rangle$ in the crystal as well as screening of the nuclear charge. See, for example, M. Tinkham, Proc. Roy. Soc. (London) **A236**, 549 (1956); and K. W. H. Stevens, *ibid.* **A219**, 542 (1953). Also see discussion of pseudofield effect in Sec. VI.

[15] S. Sugano and I. Tsujikawa, J. Phys. Soc. Japan **13**, 899 (1958).

[16] D. S. McClure, J. Chem. Phys. **36**, 2757 (1962); H. A. Weakliem and D. S. McClure, Suppl. J. Appl. Phys. **33**, 347 (1962).

[17] N. L. Laurence, E. C. McIrvine, and J. J. Lambe, J. Phys. Chem. Solids **23**, 515 (1962).

[18] S. Sugano and Y. Tanabe, J. Phys. Soc. Japan **13**, 880 (1958).

[19] S. Sugano and M. Peter, Phys. Rev. **122**, 381 (1961).

[20] R. Lacroix, Compt. Rend. **12**, 1768 (1961). R. Lacroix and G. Emeh, Helv. Phys. Acta. **35**, 592 (1963).

Eqs. (3)–(6) now became

$$\Delta g_{II}=-8\lambda_{II}'k_{II}'/\Delta_{II}, \quad \Delta g_{\perp}=-8\lambda_{\perp}'k_{\perp}'/\Delta_{\perp}, \tag{8}$$

$$D=-4[\Delta_{II}(\lambda_{II}'^2-\lambda_{\perp}'^2)+(v/2)\lambda_{II}'^2]/\Delta_{II}\Delta_{\perp}, \tag{9}$$

or

$$D=(\lambda_{\perp}'/2k')[\Delta g_{II}(\lambda_{II}'/\lambda_{\perp}')-\Delta g_{\perp}]. \tag{10}$$

Thus, we see from Eq. (9) that the sign of the ground-state splitting will be reversed if

$$\frac{\lambda_{\perp}'-\lambda_{II}'}{\lambda_{II}'}<\frac{\frac{1}{2}v}{\Delta_{II}(1+\lambda_{\perp}^{e}/\lambda_{II}^{e})}. \tag{11}$$

Since $|v|\sim 10^3\ \mathrm{cm}^{-1}$ and $\Delta_{II}\sim 15\,000\ \mathrm{cm}^{-1}$, an anisotropy of a few percent of the right sign would be enough to reverse the sign of D.

Kamimura[21] has recently suggested that such an anisotropic s-o coupling is also responsible for the reversal of the sign of D for Cu^{3+} and Ni^{2+} as well as in Cr^{3+}. He has shown how the distortion of the covalent π bonds by the trigonal field gives rise to just such an anisotropic s-o coupling of the right magnitude and sign needed to explain the reversed sign of D. Unfortunately, sufficiently precise values of $(\lambda_{II}-\lambda_{\perp})/\lambda$ cannot be calculated theoretically to enable one to use Eq. (9) to determine v from the ground-state splitting. Thus in spite of the recent advance made by Kamimura in our understanding of the factors contributing to the ground-state splitting, the precise relationship between v and D is sufficiently complex so as to prevent a reliable determination of v in orbital singlet ground states. In orbitally degenerate ground states, on the other hand, v can be determined with reasonable accuracy as described elsewhere.[3,22]

Recently, Artman has suggested that the odd components of the trigonal field which are found at the noncentrosymmetric Al site might influence the ground-state splitting. However, no detailed quantitative calculations were made.

Any or all of the above factors A to C may be the source of the sign reversal here and further work seems to be necessary to determine the exact role of each.

V. THE ENDOR SPECTRUM

Figure 7 shows the hyperfine energy levels of the Cu^{3+} ($S=1$) ions in a high externally applied field H_0. The left side of the figure illustrates schematically how the various nuclear interactions affect the electronic levels in the Paschen-Back region. The hyperfine interaction energy splits the $m_S=\pm 1$ levels into four equally spaced sublevels but the $m_S=0$ state remains fourfold degenerate. The nuclear Zeeman energy removes this degeneracy and changes the hyperfine intervals of the $m_S=\pm 1$ levels by $|g_{I(\mathrm{eff})}\beta_N H_0|$ where $g_{I(\mathrm{eff})}$ is the effective nuclear g factor[23] of the Cu nucleus in the Cu^{3+} ion. The nuclear quadrupole interaction further changes the spacing between hyperfine levels.

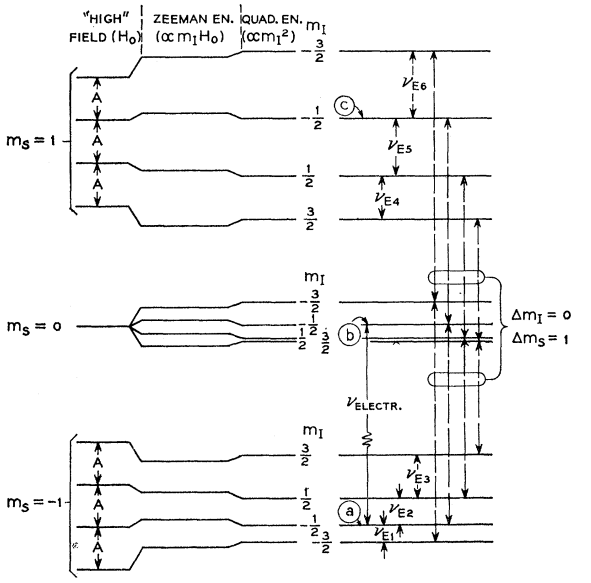

FIG. 7. The energy levels of the Cu^{3+} ion in its triplet ground state ($^3A_2$) in a magnetic field. The left portion of the figures shows the three contributions to the hyperfine splitting of the levels. In the right portion a typical electronic transition is indicated between levels a and b. When this transition was saturated, the ENDOR transitions, ν_{E1}, ν_{E2}, ν_{E5}, and ν_{E6} were observed. The dashed lines connect levels between which fast relaxation occurs. The hyperfine level spacing are exaggerated in comparison to the electronic level spacings.

The right side of Fig. 7 shows typical allowed microwave and ENDOR transitions as well as the most important relaxation processes. The microwave transitions are $\Delta m_S=1$, $\Delta m_I=0$, ENDOR transitions[24] are $\Delta m_S=0$, $\Delta m_I=1$ and the fastest relaxations occur between levels characterized by $\Delta m_S=1$, 2, $\Delta m_I=0$, with the excess angular momentum being taken up by the lattice.

If one saturates or partially saturates a microwave line (e.g., the transition ν_{electr} between levels a and b in Fig. 7) and applied a rf field H_z to the sample perpendicular to H_0 while keeping H_0 and ν_e constant, the intensity of the residual microwave line will change when H_z causes nuclear transitions between levels a or b and neighboring hyperfine levels. ENDOR transitions ν_{E1} and ν_{E2}, are of this type. Since levels a and b are connected through fast relaxation processes to level c, partial or complete saturation of ν_{electr} will result in a nonequilibrium population for level c. As a result ENDOR transitions ν_{E5} and ν_{E6} are also detected while observing the microwave line ν_e. Some of the conditions

[21] H. Kamimura, Phys. Rev. **129**, 614 (1963).

[22] A. Abragam and M. H. L. Pryce, Proc. Roy. Soc. (London) **A205**, 135 (1951); K. W. H. Stevens, *ibid.* **A219**, 542 (1953); G. M. Zverev and A. M. Prokhorov, Zh. Eksperim. i Teor. Fiz. **39**, 57 (1960) [translation: Soviet Phys.—JETP **12**, 41 (1961)]. See also reference 3.

[23] J. N. Baker and B. Bleaney, Proc. Roy. Soc. (London) **A245**, 156 (1958).

[24] G. Feher, Phys. Rev. **103**, 83 (1956).

necessary for the observability of ENDOR transitions such as ν_{E1} and ν_{E2} are

$$(a): \quad g\beta H_1(T_1T_2)^{1/2}>1. \tag{12}$$

H_1 is the microwave field and T_1 and T_2 are the electron spin-lattice and phase memory relaxation times. This condition must be satisfied to saturate ν_e.

$$(b): \quad g_I\beta_N H_{2\,\mathrm{eff}}(T_1T_2)^{1/2}>1 \tag{13}$$

$H_{2\,\mathrm{eff}}$ is the effective rf field and this inequality must be satisfied in order that the ENDOR transition rate may exceed the electronic relaxation rate. $H_{2\,\mathrm{eff}}$ exceeds the applied H_2 by a factor of order of magnitude $m_SA/g_I\beta_NH_0$ where A is the hyperfine energy and m_S is the electronic magnetic quantum number. T_2 appears in Eqs. (12) and (13) because spin diffusion in the microwave line which proceeds at a rate T_2^{-1} provides a statistically independent relaxation mechanism from the spin-lattice mechanism.

Different conditions must be fulfilled to observe the ENDOR lines between levels whose m_S is different from those connected by the microwave transition (such as ν_{E5} and ν_{E6}):

$$g_I\beta_N H_{2\,\mathrm{eff}}T_1>1, \tag{14}$$

$$T_1 \quad \text{not} \quad \gg T_2. \tag{15}$$

The first of these conditions differs from the inequality (13) in that T_2 does not appear. The change of population of level c proceeds by relaxation from a level (a or b) of equal width and not by saturation with monochromatic radiation and therefore depends only on T_1. If (13) is fulfilled, this condition is always met. The second condition, that T_2 be of the same order of magnitude as T_1, ensures that level a or b is sensitive to relaxation from level c which proceed with relaxation time T_1. If $T_1\gg T_2$, population changes caused by ENDOR transition involving level c would have little effect on the population of levels a or b.

The strongest ENDOR lines were observed by using the low-field microwave transitions. The microwave lines were 20 Oe or 56 Mc/sec in width and lines from Cu^{63} and Cu^{65} could not be resolved. The ENDOR lines occurred at about 200 Mc/sec and had a width of 60 kc/sec and thus are about 10^{-3} of the microwave linewidth. This made it possible to resolve the hyperfine lines arising from the two copper isotopes and to determine the hyperfine interaction constants to high precision.

TABLE II. Values of $\langle 1/r^3\rangle$ in atomic units for Cu^{2+} and Cu^{3+}.

	Free Ion	Crystal
Cu^{3+}	9.018[a]	6.6±2.0[b]
Cu^{2+}	8.251[a]	6.3[c]

[a] Calculated by G. Burns (to be published) using wave functions given by R. W. Watson, Phys. Rev. 118, 1036 (1960).
[b] Results of present work.
[c] B. Bleaney, K. D. Bowers and M. H. L. Pryce, Proc. Roy. Soc. (London) A228, 166 (1955).

TABLE III. Separation between nuclear magnetic substates as measured by ENDOR compared with values calculated using parameters of Table IV. $\theta=0°$; $m_s=0\leftrightarrow 1$.

	$m_s=-1$ ν_E (Mc/sec)		$m_s=+1$ ν_E (Mc/sec)		
$m_I\leftrightarrow m_I'$	calc	obs	calc	obs	m_I
		Cu^{63}			
$-\frac{3}{2}\leftrightarrow-\frac{1}{2}$	183.963	0.966	198.508	0.508	$-\frac{3}{2}$
	0.903	0.902	0.607	0.606	$-\frac{1}{2}$
$-\frac{1}{2}\leftrightarrow-\frac{1}{2}$	185.155	0.151	201.267	0.265	$-\frac{1}{2}$
	0.086	0.085	0.323	0.325	$\frac{1}{2}$
$\frac{1}{2}\leftrightarrow\frac{3}{2}$	186.359	0.359	204.064	0.066	$\frac{1}{2}$
	0.269	0.268	0.083	0.082	$\frac{3}{2}$
		Cu^{65}			
$-\frac{3}{2}\leftrightarrow-\frac{1}{2}$	196.885	0.883	212.539	0.543	$-\frac{3}{2}$
	0.820	0.821	0.652	0.651	$-\frac{1}{2}$
$-\frac{1}{2}\leftrightarrow\frac{1}{2}$	198.272	0.276	215.680	0.680	$-\frac{1}{2}$
	0.205	0.203	0.740	0.739	$\frac{1}{2}$
$\frac{1}{2}\leftrightarrow\frac{3}{2}$	199.684	0.685	218.872	0.871	$\frac{1}{2}$
	0.590	0.587	0.885	0.886	$\frac{3}{2}$

VI. RESULTS

The hyperfine constants were determined by diagonalizing the 12×12 secular determinant which is obtained from the spin Hamiltonian (1) with various values for the parameters A, B, $g_{I(\mathrm{eff})}$ and e^2qQ and the observed values of H_0 until the computed ENDOR frequencies agreed with all the observed ones to within a few kc/sec. Table II shows the final fit between the theoretical and experimental values of ν_E. In this way we obtained the results shown in Table III. From these results one calculate the ratios of the hyperfine structure parameters for the two copper isotopes in the Cu^{3+} ion and compare them with the corresponding ratios for the isotopes in the neutral atom. This comparison is shown in Table IV.

VII. DISCUSSION

The physical significance of these results are now discussed.

1. A

The great precision to which A was obtained is not in itself of considerable significance though the precise ratio of A for the two isotopes is very useful as will be discussed in the next section.

The sign of A is found to be negative, indicative of

TABLE IV. Hfs, quadrupole coupling, and $g_{I(\mathrm{eff})}$ of Cu^{63} and Cu^{65} as determined from ENDOR.

	Cu^{63}	Cu^{65}
A (Mc/sec)	−192.947±0.001	−206.679±0.001
B (Mc/sec)	−180.10 ±0.05	−192.916±0.05
e^2qQ (Mc/sec)	−0.168±0.004	−0.142±0.004
$g_{I\parallel(\mathrm{eff})}$ (Mc/sec/10^4 Oe)	11.383±0.002	12.195±0.002

TABLE V. Cu^{63}/Cu^{65} hyperfine structure anomaly and quadrupole moment ratio.

	$Cu^{3+}(d^8)$[a]	Other Cu measurements	
A^{63}/A^{65}	0.933559±8	0.933567±2	At. beams[b] ($4s^1$)
g^{63}/g^{65}	0.9334 ±3	0.933424±19	NMR[c] ($3d^{10}$)
$\Delta^{63,65}$ (percent)[d]	0.0145 ±8	0.0153 ±2	($4s'$)
Q^{63}/Q^{65}	1.10 ±4	1.0807 ±2	Quad. res.[e] ($3d^{10}$)
		1.08 ±2	EPR[f]

[a] Present experiment.
[b] Y. Ting and H. Lew, Phys. Rev. **105**, 581 (1957).
[c] H. E. Walchli, Oak Ridge National Laboratory Report ORNL-1469 (unpublished), Suppl. II.
[d] The quoted error in Δ ignores the error in g^{63}/g^{65} since that is the same for $\Delta(s_{1/2})$ and $\Delta(d^8)$ and its inclusion would obscure the similarity of these Δ's. The experimental error of each Δ is in fact ±0.002%.
[e] H. Kruger and U. Meyer-Berkhout, Z. Physik. **132**, 171 (1952).
[f] B. Bleaney, K. D. Bowers, and M. H. L. Pryce, Proc. Roy. Soc. (London) **A228**, 166 (1955).

exchange polarization of the inner s electrons by exchange with the d electrons.[25] The contribution of the orbital hyperfine field, while smaller than the core polarization is not negligible and will be discussed in a future publication.

The value of the hyperfine field is −160 000 G per unit electron spin (i.e., for 2 Bohr magnetons) and is of the order of a few percent of that due to a single unpaired s electron on the neutral copper atom.[26] It is also of the same sign and similar in magnitude to the isotropic hyperfine field per unit electron spin found for other $3d$ transition metal ions.

2. A^{63}/A^{65}

The ratio A^{63}/A^{65} yields together with g^{63}/g^{65} a value for the hyperfine structure anomaly[27] Δ. Δ is defined as $(A^{63}/A^{65})(g^{65}/g^{63})-1$ and arises from a difference in the magnetization distributions in the two nuclei. Appreciable values of Δ for $Z\lesssim 50$ are obtained only if A arises for $s_{1/2}$ electrons.[28] p electrons are only 3% as effective as s electrons in contributing to Δ for $Z=29$ and the effect of electrons with $l>1$ is negligible.

The hyperfine anomaly for $Cu^{63,65}$ has been measured by atomic beam experiments[26] and was found to be $\Delta(s_{1/2})=0.0153\pm 0.0002\%$. This is a very low value reflecting the great similarity of the nuclear magnetic structure of the two isotopes. Table IV compares this result with the present experiment. We find that $\Delta(d^8)=0.0145\pm 0.0008\%$ so that very nearly $\Delta(s_{1/2})=\Delta(d^8)$.

We can use this measurement to estimate the fractional contribution of unpaired $s_{1/2}$ electrons to the total hyperfine interaction A for the d^8 configuration of the Cu^{3+}. Let us write this fraction $f=A_{s_{1/2}}(d^8)/A_{\text{tot}}(d^8)$. We can then, on the basis of the discussion in the preceding paragraph, split up the contributions to the hyperfine structure anomaly $\Delta(d^8)$ into s and p parts neglecting all higher angular momentum electronic wave functions:

$$\Delta(d^8)=f\Delta(s_{1/2})+(1-f)(0.03)\Delta(s_{1/2}). \tag{16}$$

Using the experimental values with their uncertainties for $\Delta(s_{1/2})$ and $\Delta(d^8)$ given above, we can solve this equation and find that $f=0.95\pm 0.08$. This again confirms that the hyperfine interaction $A(d^8)$ arises largely from $s_{1/2}$ electron wave functions which is a manifestation of core polarization[25] in atoms with partially filled d or f shells.

It might be thought that such hyperfine structure anomaly measurements could be used to determine those s shells which are principally responsible for the hyperfine interaction. This is, however, not the case since $\Delta(s_{1/2})$ is independent of the principal quantum number, because the shape of all s-wave functions inside the nucleus is the same for any given Z.

3. Pseudofield Effect

The $\mathbf{H}_0\cdot\mathbf{I}$ term in the spin Hamiltonian reflects the direct interaction of the external magnetic field with the nuclear magnetic moment. Baker and Bleaney[23] pointed out an additional term of the same form which results in the nucleus seeing an effective external magnetic field $H_0(1+\delta)$ where, as will be shown, δ is approximately 1% for orbital singlet ground states.

In the expression for the energy of a paramagnetic ion, from which the spin Hamiltonian is deduced by perturbation theory, there appear terms of the type

$$P\mathbf{L}\cdot\mathbf{I}+\beta\mathbf{H}\cdot(\mathbf{L}+2\mathbf{S})+\lambda\mathbf{L}\cdot\mathbf{S}. \tag{17}$$

Here $P=2g_I\beta\beta_N\langle r^{-3}\rangle$ and $P\mathbf{L}\cdot\mathbf{I}$ expresses the interaction between the electronic orbital magnetic moment and the nuclear moment. The second and third terms are the electronic Zeeman energy and the spin-orbit coupling, respectively. As the ground state of Cu^{3+} in the crystal is an orbital singlet, $P\mathbf{L}\cdot\mathbf{I}$ and $\lambda\mathbf{L}\cdot\mathbf{S}$ vanish in first order. However, the second-order interaction with excited states introduces cross terms of the type

$$-2\lambda\beta S_iH_j\sum_n\frac{\langle 0|L_i|n\rangle\langle n|L_j|0\rangle}{E_n-E_0}=-2\lambda\beta S_iH_j\Lambda_{ij}, \tag{18}$$

$$-2\beta PI_iH_j\sum_n\frac{\langle 0|L_i|n\rangle\langle n|L_j|0\rangle}{E_n-E_0}=-2\beta PI_iH_j\Lambda_{ij}. \tag{19}$$

In (18) and (19) the sum extends over the excited orbital levels. Further details are given in Pryce's original paper.[29]

Equation (18) gives rise directly to the familiar g-shift tensor of singlet states, i.e.,

$$(\Delta g)_{ij}=-2\lambda\Lambda_{ij}. \tag{20}$$

[25] V. Heine, Phys. Rev. **107**, 1002 (1957). J. H. Wood and G. W. Pratt, Jr. *ibid.* **107**, 995 (1957); R. E. Watson and A. J. Freeman, *ibid.* **123**, 2027 (1961). This last reference should be consulted for a more complete bibliography of the problem.
[26] Y. Ting and H. Lew, Phys. Rev. **105**, 581 (1957).
[27] A. Bohr and V. F. Weisskopf, Phys. Rev. **77**, 94 (1950).
[28] J. Eisinger and V. Jaccarino, Rev. Mod. Phys. **30**, 528 (1958).
[29] M. H. L. Pryce, Proc. Phys. Soc. (London) **A63**, 25 (1950).

Equation (19) represents the mixing into the ground state of some orbital magnetic moment by the external magnetic field and the subsequent magnetic interaction between this orbital magnetic moment and the nuclear moment. This is part of the "chemical shift" familiar in nuclear magnetic resonance. Expression (19) may be rewritten in terms of the electronic g shift given by Eq. (20), as

$$\frac{2g_I\beta_N\beta^2(\Delta g)_{ij}}{\lambda}\left\langle\frac{1}{r^3}\right\rangle I_iH_j. \tag{21}$$

Thus, the apparent fractional change in the external magnetic field seen by the nucleus, δ, may be written for axial symmetry as

$$\delta_{\parallel,\perp}=-\frac{2\beta^2(\Delta g_{\parallel,\perp})}{\lambda}\left\langle\frac{1}{r^3}\right\rangle. \tag{22}$$

In using Eq. (22) to determine $\langle 1/r^3\rangle$, we must use a value of λ that takes into account covalency and other effects in the crystal which change λ from its free-ion value. The reductions of the spin-orbit coupling, ξ, and the components of angular momentum $\mathbf{l}$ in the crystal are usually expressed in the following way:

$$\xi'=\langle t_2|\,\xi\mathbf{l}\cdot\mathbf{s}\,|e\rangle, \tag{23}$$

$$k'=\langle t_2|\,\mathbf{l}_z\,|e\rangle, \tag{24}$$

where $\xi\mathbf{l}\cdot\mathbf{s}$ and $\mathbf{l}$ are the single electron operators of the s-o interaction and angular momentum, respectively. When t_2 and e are pure d orbitals, $\xi'=\xi$ and $k'=1$. ξ', if so defined, includes the effects of the orbital reduction. It is convenient for our purposes to separate this effect on ξ'; we write $\xi''=\xi'/k'$, where ξ'' now expresses only the reduction of $\langle 1/r^3\rangle$ and the modification of the effective nuclear charge in the crystal. The effective, s-o coupling constant, λ_{eff}, defined in terms of the electronic g shift, (i.e., $\Delta g\sim 8\lambda_{\text{eff}}/10Dq$), can therefore be written as

$$\lambda_{\text{eff}}=\lambda''(k')^2, \tag{25}$$

where $\lambda''=\xi''/3$. If these effects are taken into account in Eqs. (18) and (19), then $\lambda_{\text{eff}}/(k')^2$ should be used for λ in Eq. (22). Substituting the experimentally determined parameters into Eq. (22) we find

$$\langle 1/r^3\rangle=[1/(k')^2]4.26 \text{ atomic units}. \tag{26}$$

Unfortunately, we have no independent method of accurately determining k'. While values of k' as small as 0.7 have been estimated in the literature,[19] we believe this to be too small. For example, in the case of orbitally degenerate ground states in the more covalent $4d$ and $5d$ series one finds values of k that range between 0.85 and 1.0.[30] While k is the orbital reduction within a t_2 orbital, it is generally assumed that $k\sim k'$. If we choose $k'\sim 0.8\pm 0.1$, then for Cu^{3+} $\langle 1/r^3\rangle=6.6\pm 1.0$ a.u. This value is given in Table II along with the value of $\langle 1/r^3\rangle$ for Cu^{2+} in a crystalline environment as well as the free-ion values for these ions.

We believe, however, that uncertainties involved in estimating such parameters as k', should lead one to be careful in trying to draw conclusions from this table regarding the degree of reduction of $\langle 1/r^3\rangle$ in the crystal for these two ions. Shulman and Sugano[31] have indicated they find virtually no reduction in $\langle 1/r^3\rangle$ for Ni^{2+} in an analysis of the fluorine hfs in NiF_2.

This pseudofield effect is much larger for ions which have very low-lying excited states such as are found in Co^{2+}. From the ENDOR spectrum of Co^{2+} in MgO, Fry, Llewellyn and Pryce[32] found the pseudofield effect to be about 40%. Similarly in the rare earths where one has very low-lying excited states in the pseudofield effects will be very large.[32,33]

4. The Nuclear Electric Quadrupole Energy

The observed value of the quadrupole interaction energy $e^2qQ(Cu^{63,65})$ reflects the magnitude of the electric field gradient at the nucleus of the Cu^{3+} ion in Al_2O_3 and the magnitude of the nuclear electric quadrupole moment $Q(Cu^{63,65})$. The value of q can be compared to the field gradient which has been measured for other ions in the same lattice site. The most direct comparison would be one to the gradient at the Al nucleus which has been measured by Pound.[34] Using nuclear magnetic resonance he obtained $e^2qQ(\text{Al})=2.393$ Mc/sec. The electric field gradient for the Al^{3+} site was calculated on the basis of a point-charge model by Bersohn.[35] This calculation leads to a value for $e^2qQ(Al^{27})=0.43$ Mc/sec for the bare nucleus. Using an antishielding factor[36] $\gamma(Al^{3+})=-2.6$ the measured value of $e^2qQ(Al^{3+})$ would be expected to be 1.6 Mc/sec, which is about half of the observed energy. The remaining energy is ascribed to the field gradient arising from covalent binding of the Al^{3+} ion.

In attempting a similar calculation for the Cu^{3+} ion in the same site we obtain for the bare Cu^{63} nucleus a value of $e^2qQ(Cu^{63})=0.46$ Mc/sec. Here we used 0.159×10^{-24} cm^2 for $Q(Cu^{63})$.[37] A value for $\gamma(Cu^{3+})$ may be estimated from a knowledge of $\gamma(Cu^{+})$ which has been calculated to be -15 by Sternheimer and Foley[38] and observed to be -16.5 by Krueger and Meyer-Berkhout.[39] The more positively charged Cu^{3+}

[30] See Stevens' paper in reference 14; in addition, Tinkham's paper quoted in reference 14 cites values of $k'>0.9$.

[31] R. G. Shulman and S. Sugano (private communication).

[32] D. J. I. Fry, P. M. Llewellyn, and M. H. L. Pryce, Proc. Roy. Soc. (London) **A266**, 84 (1962).

[33] D. Halford, C. A. Hutchison, Jr., and P. M. Llewellyn, Phys. Rev. **110**, 284 (1958); R. J. Elliot, Proc. Phys. Soc. (London) **B70**, 119 (1957).

[34] R. V. Pound, Phys. Rev. **79**, 689 (1950).

[35] R. Bersohn, J. Chem. Phys. **29**, 326 (1956).

[36] T. P. Das and R. Bersohn, Phys. Rev. **102**, 733 (1956).

[37] B. Bleaney, K. D. Bowers, and M. H. L. Pryce, Proc. Roy. Soc. (London) **A228**, 166 (1955).

[38] R. M. Sternheimer and H. M. Foley, Phys. Rev. **102**, 731 (1956).

[39] H. Krueger and V. Meyer-Berkhout, Z. Physik **132**, 171 (1952).

ion is expected[40] to have a somewhat smaller antishielding factor and we assume $\gamma(Cu^{3+})\approx 5$. In this way we calculate for Cu^{3+} in Al_2O_3 a quadrupole interaction energy of 2.8 Mc/sec. This is nearly two orders of magnitude greater than the observed value of 0.042 Mc/sec. We have been unable to find a satisfactory explanation for this difference but will briefly discuss some effects which may be responsible for it.

The most important difference between the Cu^{3+} and Al^{3+} ions used in the comparison above is that the Cu^{3+} ion has a partially filled d shell ($3d^8$). The paramagnetic resonance spectrum shows that the two d holes form a $^3A_2$ ground state which produces no electric-field gradient at the nucleus. Thus, there are no first-order contributions to e^2qQ from the unfilled d shell. Second-order effects arising from the admixture of other orbitals as a result of the crystal field or applied magnetic field have been estimated[41] to be small.

Antishielding factors have only been calculated and measured for ions with spherically symmetrical charge distributions and the values of $\gamma(Cu^{+})$ quoted above are of this type. It is possible that the nonspherically symmetrical charge distribution of Cu^{3+} has a radically different antishielding factor. It is even conceivable that the d^8 configuration produces at the nucleus a considerable shielding of external electric field gradients.[42]

Another reason for the small value of the observed electric quadrupole energy for Cu^{3+} may be that the ion is displaced along the c axis from the normal Al position sufficiently to lower the electric field gradient almost to zero. (The Cu^{3+} ion is not at a center of symmetry.) But such a displacement would also lower the axial field splitting, Dq, of the ion. The measured value of this parameter, however, was seen to fit in with the observed value of D for Ni^{2+}, and its general magnitude implies a reasonably large axial field. We, therefore, do not consider such lattice distortions in the vicinity of the Cu^{3+} which undoubtedly occur to some extent as the likely explanation of this anomaly.

ACKNOWLEDGMENTS

We wish to thank D. Linn, B. Szymanski, and E. W. Kelly for their experimental assistance; J. P. Remeika for growing the single crystals of Cu^{3+}-doped Al_2O_3; D. L. Wood for help with the optical spectrum; and R. Bersohn, A. M. Clogston, V. Jaccarino, H. Kamimura, M. Peter, R. G. Shulman, and R. E. Watson for many helpful discussions.

[40] E. G. Wikner (private communication).
[41] R. Bersohn (private communication).
[42] Conversations with G. Burns and E. G. Wikner lead us to consider this an unlikely possibility.

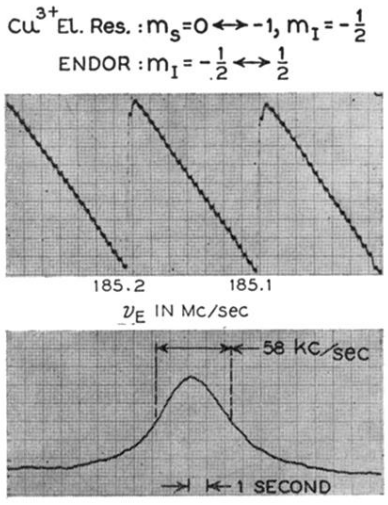

FIG. 2. The lower trace shows the ENDOR line corresponding to the transition $m_I = -\frac{1}{2} \rightarrow +\frac{1}{2}$ for the electronic level $m_s = -1$. The upper trace shows the analog of the rf frequency applied to the sample. The two traces were obtained simultaneously on a two-channel recorder.

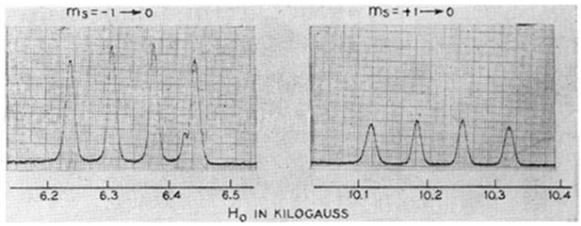

FIG. 4. Observed spectrum of Cu^{3+} at 1.8°K. The greater intensity of the low-field lines establishes the negative sign of D. At room temperature, the high- and low-field sets of lines had the same intensity. The weak line at 6.43 kG is due to iron impurities.